Chapter 8
Selective Removal of Nitrate and Phosphate from Wastewater Using Nanoscale Materials

T.K.M. Prashantha Kumar, Trivene R. Mandlimath, P. Sangeetha, S.K. Revathi, and S.K. Ashok Kumar

Abstract Excessive nitrogen (N) and phosphorous (P) release into runoff from human activities is a major cause of eutrophication, which degrades freshwater and ecosystems. Phosphate and nitrate pollutants can be removed by chemical precipitation, biological treatment, membrane processes, electrolytic treatment, ion-exchange and adsorption process to remove these pollutants from water sources effectively. Adsorption is a cost-effective solution for efficient nitrate and phosphate ions removal. In this review various nanoscale adsorbents such as zero-valent metal, metal oxides, functionalized materials and carbon-based materials are surveyed. Their adsorption capacities under various conditions are compared.

Keywords Eutrophication • Nanomaterials • Nitrate • Phosphate • Composite materials

Abbreviations

BOD	Biochemical Oxygen Demand
C-cloth	Carbon cloth
CNT	Carbon nanotube
COD	Chemical Oxygen Demand
DNA	Deoxyribonucleic acid
EDTA	Ethylenediamine tetracetic acid

T.K.M. Prashantha Kumar • T.R. Mandlimath • P. Sangeetha • S.K. Ashok Kumar (✉)
Department of Chemistry, School of Advanced Sciences, VIT University,
Vellore 632014, Tamil Nadu, India
e-mail: ashokkumar.sk@vit.ac.in

S.K. Revathi
Department of Chemistry, Nandi Institute of Technology and Management Sciences,
Bengaluru 560001, Karnataka, India

S. Ranjan et al. (eds.), *Nanoscience in Food and Agriculture 3*,
Sustainable Agriculture Reviews 23, DOI 10.1007/978-3-319-48009-1_8

G-nZVI	Graphene-supported nanoscale zero-valent iron
HZO	Nano-hydrous zirconium oxide
IEP	iso electric point
La-ZFA	Lanthanum hydroxide-Zeolite
MZVI	micro-ZVI
NOAA	National oceanic and atmospheric association
nZVI	Nanoscale zero-valent iron
OMM	Ordered mesoporous materials
ppm	Parts per million
RO	Reverse osmosis
SBA	Santa Barbara Amorphous
TDS	Total dissolved solids
USEPA	U.S. Environmental Protection Agency
WHO	World health organization

8.1 Introduction

Water played a crucial part in the origin of life and it still has an essential role in maintaining plant and animal life. Plants depend on water for the transfer of nutrients and for photosynthesis. Nearly all the processes essential for life depend on reactions that take place in an aqueous solution, be it the division of DNA in a cell, the digestion of food stuffs in the stomach or the transport of oxygen around the body (Wardlaw 2012; Nandita et al. 2015; Shivendu et al. 2014). Given an importance of water, it is not surprising that human can survive very much longer without food that they can't without water. Historically, availability of water supplies has determined where villages, towns and cities are located. Nomadic peoples and animals, may travel hundreds of miles over the course of a year following the seasonal variation in rainfall. A lack of good quality drinking water and water for sanitation brings deadly diseases such as typhoid (Schlipkoter and Flahault 2010). All these factors and many more, make water a material of great importance. The starting point of water pollution occurs when rain drops fall through the atmosphere they dissolve small quantities of gases in the atmosphere. Where there is little air pollution, the gases are mainly nitrogen, oxygen and a little carbon dioxide does make the water very slightly acidic owing to the production of weak carbonic acid. Rain falling in a thunderstorm is more acidic than normal. The energy of the lightning is sufficient to dissociate nitrogen molecules, which then combine with oxygen to give oxides such as nitrogen dioxide (Schumann and Huntrieser 2007). Once rain water contact with land surface, water pollution begins slowly depending upon distanced travelled by water, there may be following types of impurities present in the water (APHA 1985):

(i) Dissolved impurities: The following impurities may be present in the water in the dissolved form:

Table 8.1 Water quality parameters

Physical parameters	Chemical parameters	Biological parameters
Colour	Dissolved oxygen	Bacteria (pathogenic)
Odour	Biochemical oxygen demand	Coliforms and other bacteria
Turbidity	Chemical oxygen demand	Algae
Conductivity	pH, alkalinity	Viruses
Solids	Ammonia, nitrates, nitrites, sulphates, phosphates chlorides, silica, calcium, magnesium, hardness, sodium, potassium, iron, heavy metals, detergents, and pesticides	

- Inorganic salts: cations like Ca^{2+}, Mg^{+2}, Na^{+}, K^{+}, Fe^{+2}, Cu^{+2}, Al^{+3} and anions like Cl^{-}, SO_4^{2-}, HCO_3^{-}, NO_3^{-}, PO_4^{3-} and sometimes F^{-} and NO_2^{-}
- Organic salts: drugs and dyes
- Dissolved gases: O_2, CO_2, NOx and SOx and sometimes NH_3 and H_2S
- Toxic elements: Like Hg^{2+}, As^{5+}, Cr^{6+}, Pb^{2+}, Cd^{2+} etc

(ii) Colloidal impurities: clay, silica, $Al(OH)_3$, $Fe(OH)_3$, humic acids, etc.
(iii) Suspended impurities: Inorganic matters (clay and sand) while organic matters (oils globules, vegetables and animal matter)
(iv) Biological impurities: Bacteria and micro-organism (virus, algae, fungi and diatoms)

8.1.1 Water Quality

The treatment of water in order to make it suitable for drinking, domestic or industrial use includes a physical, chemical and biological methods which change an initial composition of water. Water treatment involves not only purification and removal of various unwanted and harmful impurities, but also improvement of the natural properties of water by adding certain deficient ingredients. Water quality parameters based on the present-day standards and guidelines are presented to assist in the establishment of water system performance goals for any plant. The water quality parameters are generally divided into three categories like physical, chemical and biological (Pfafflin and Ziegler 2006). These parameters are briefly summarized in Table 8.1.

The standards for drinking water quality are typically set by governments or by international standards (WHO 1997). These standards usually include minimum and maximum concentrations of contaminants, depending on the intended purpose of water use. Visual inspection cannot determine if water is of appropriate quality. Simple procedures such as boiling or the use of a household activated carbon filter are not sufficient for treating all the possible contaminants that may be present in

water from an unknown source. Even natural spring water considered safe for all practical purposes in the nineteenth century must now be tested before determining what kind of treatment, if any, is needed. Chemical and microbiological analysis, while expensive, are the only way to obtain the information necessary for deciding on the appropriate method of purification (Droste 1998).

8.1.2 Nitrate and Phosphate Pollution

The nitrate and phosphate substances are among the most problematic pollutants which significantly affecting the surface and groundwater all around the world. However, the nitrate and the phosphate pollution has been neglected by many countries. The rapid development of industrial and agricultural activities have take over the human awareness on the effects of nutrients pollution to us and to the environments. Considering the bad effects of phosphate and nitrate pollution, WHO permits 5 mg/L as the maximum level of phosphate whereas for nitrate not more than 10 mg/L that is safe in drinking water (WHO 1985). Common causes of phosphate toxicity in humans include impaired renal function, rhabdomyolysis and tumourlysis syndrome. In addition, exogenous phosphate toxicity is also documented in patients with Hirschsprung disease when exposed to hypertonic phosphate enemas (Razzaque 2011). When human consume high concentration of nitrate through contaminated drinking water, there is high risks of being infected by diseases like methaemoglobinemia, gastric cancer and non-Hodgkin's lymphoma (APHA 1998; Rademacher et al. 1992). Besides, the long term exposure to nitrates and nitrites at level above maximum contamination level will cause diseases like diuresis, increased starchy deposits and hemorrhaging of the spleen (EPA 1990). Hence, the removal of nitrate and phosphate from wastewater prior to discharge is now necessary. Several methods are being used to remove nitrate and phosphate ions. The present review articles deals with the current techniques for the nitrate and phosphate ions removal from waste water (Fig. 8.1).

8.2 Methods of Nitrate and Phosphate Removal

Traditional methods for nitrogen removal from waste water are biological denitrification processes, ion exchange, reverse osmosis, electrodialysis, and chemical denitrification. Among these methods, the first four methods have been applied in industry. Each of these technologies has its own strengths and drawbacks and their feasibility depends on the various factors such as cost, water quality improvement, residuals handling, and post-treatment requirements.

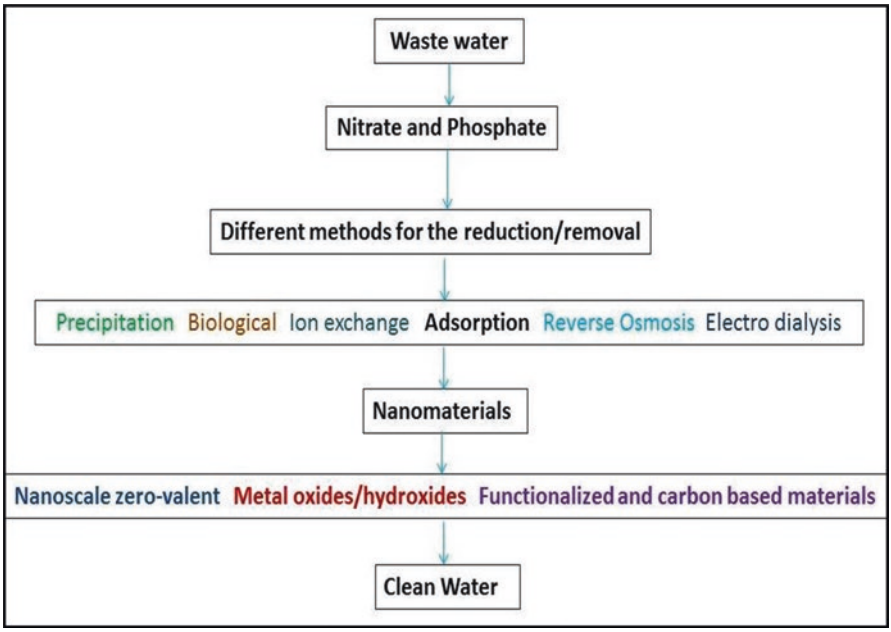

Fig. 8.1 Treatment technologies for the reduction of nitrates and phosphates in wastewater

8.2.1 Biological Denitrification Process

In this process, nitrate is converted to nitrogen gas by denitrifying bacteria in the absence of oxygen ($NO_3 \rightarrow NO_2 \rightarrow NO \rightarrow N_2O \rightarrow N_2$). In order to satisfy the growth and energy requirements of the bacteria, methanol in excess of 25–35 % must be added as a source of carbon. The removal efficiency ranges from 60 to 95 %. The major advantage to anaerobic denitrification is that there are no waste products requiring disposal, produces a non-toxic by product (N_2), suitable for large applications, can handle high concentrations, and destructive method. The nitrate removal from wastewater by the biological denitrification technology using immobilized *Psuedomonas Stutzeri* bacteria in a fluidized bed bio reactor with different initial nitrate concentrations (150, 180 and 200 ppm) and found that the nitrogen removal efficiency achieved was highest (96 %) with methanol as carbon source, followed by ethanol (77 %) and methane (70 %) during the period 6–8 h (Srinu and Setty 2011). The influence of low-intensity ultrasound to biological denitrification for nitrate removal from synthetic wastewater (Xie and Liu 2010). They used ethanol as the carbon source and showed that the ultrasonic intensity of 0.2 Wcm^{-2} and irradiation time of 10 min may be the most effective and economical ultrasonic parameters to enhance the efficiency of biological nitrogen removal processes. Some of the disadvantages of this method like electron donor and carbon source required, requires downstream treatment (e.g., ozonation), high-maintenance, long start-up times, pH temperature sensitive and membrane fouling.

8.2.2 Ion Exchange Process

In the Ion exchange process (IEP), wastewater is passed through a media bed which removes both anionic phosphorus and anionic nitrogen ions and replaces them with another ion from the media. The exhausted resin will be regenerated using a concentrated solution of brine. Besides, this technique found to be stable, quick removal, easily automated, cost-effective, low maintenance and non-destructive. Difficulties in the process may be caused by fouling of the IE resin due to organic backbone and reduction in the exchange capacity due to sulphates and other ions. The efficiency and cost of nitrogen and phosphorus removal by IE depends largely on the degree of pre-treatment and the quality of the water to be treated. Removal of nitrogen and phosphorus contents ranges from between 80 to 92 % using strong base anion resins (Amberlite IRA-410). Several resins have been tested for nitrate removal from ground water such as strong base anion exchange resin Purolite A 520E with column (Samatya et al. 2006). The total capacity was calculated to be 157 mg NO_3^- per gram resin and the column utilization efficiency was about 81 %. They used 0.6 M NaCl to elute nitrate loaded on resin and elution efficiency was about 96 %. Equilibrium and kinetic parameters for the removal of nitrate ions from aqueous solutions on Amberlite IRA 400 resin and maximum adsorption capacity was found to be 769 mg NO_3^- per gram at 25 °C (Chabani et al. 2006).

8.2.3 Reverse Osmosis

In reverse osmosis (RO), water begins to flow in the reverse direction with the application of pressure (750 psi) higher than the value of osmotic pressure. The pressure required to force the permeation through the membrane is dictated by the osmotic pressure of the feed stream. Membranes are generally made of materials such as cellulose acetate, polyamides and composite materials. In actual practice the process has been beset with difficulties primarily due to membrane fouling, expensive energy, large capital costs and requires treatment or disposal of concentrate. In addition, some nitrate and phosphate ions escape through the membrane (efficiency about 65–95 %). Advantages of this technique are good for waters with high TDS content, no by products, non-destructive**.** A comparison between three technologies RO, IE and biological process for nitrate removal has been studied (Darbi et al. 2003). They showed that the lowest nitrate removal efficiency was obtained with RO (85 %) with compared to 90 and 96 % for IE and biological process, respectively. The RO could be very effectively applied for water desalination and water denitrification in a rural area (Schoeman and Steyn 2003). They showed that the nitrate-nitrogen was reduced from 42.5 mg/L in the RO feed to only 0.9 mg/L in the RO product water (98 % removal). Removal of ammonium and nitrate from mine water by using RO and the retention of nitrate was reported to be more than 90 % (Hayrynen et al. 2009) during the concentration. In another study (Richards et al.

2010) carried out to evaluate the impact of pH on retention of nitrate by reverse osmosis (RO) and reported that the nitrate retention depended on membrane types, and was mostly pH independent.

8.2.4 Electrodialysis

Like reverse osmosis, electrodialysis (ED) is a non-selective demineralization process which removes all ions which would include the nitrate and phosphate ions. ED is accomplished by making cation and anion from aqueous solutions pass through IE selective membranes using the driving force of an electric field. When electric current is applied, the cations pass through the cation-exchanging membranes in one direction and the anions pass through the anion-exchanging membranes in the other direction (Hell et al. 1998). Disadvantages in the operation of this process include membrane clogging and precipitation of low-solubility salts of the membrane. Acidification of the water and removal of some of the solids prior to treatment has been effective in minimizing these problems and it adds to the cost. Removal efficiency ranges from between 30 to 50 % (for nitrogen). Removal of nitrate in Moroccan groundwater carried out by ED using different types of anion exchange membranes with one type of cation exchange membrane to treat water containing 113 mg/L of nitrate (El Midaoui et al. 2001 and 2002). They found that the content of nitrate was reduced to 30 mg/L after 1 h of ED operation. Considering the effect of pH, the study showed 3 and 5 were the most effective operating condition for the separation of nitrate from aqueous solutions using ED and the concentration of nitrate was reported to decrease from 173.8 mg/L to 4–5 mg/L after 42 min of operation (Abou-Shady et al. 2012).

8.2.5 Chemical Precipitation

Chemical precipitation is a flexible technology allowing for application of the metal salts at several stages during wastewater treatment (EPA 2000; Jenkins et al. 1971; Jiang and Graham 1998). Precipitation of phosphorus in wastewater may be accomplished by the addition of such coagulants as lime, alum, ferric salts and polyelectrolytes either in the primary or secondary state of treatment, or as a separate operation in tertiary treatment. In general, large doses in the order of 200–400 ppm of coagulant are required. However, subsequent coagulation and sedimentation may reduce total phosphates to as low as 0.5 ppm, as in the case of lime. Doses of alum of about 100–200 ppm have reportedly reduced orthophosphates to less than 1.0 ppm. Phosphorus removal by chemical coagulation generally is efficient with removals in the order of 90–95 % reported. Additional benefits are gained in the process by a reduction in BOD to a value of less than 1.0 ppm. Both installation and chemical costs are high, however, and the sludges produced are both voluminous

and calculations of accurate dosages of chemicals are impossible because of changing levels of alkalinity, different competitive reactions and other factors.

8.3 Adsorption

Adsorption was first observed by C.W. Scheele in 1773 for gases, followed by Lowitz's experiments in 1785 for solution (Kraemer 1930). Adsorption is the accumulation of a substance at a surface or the interface between two phases. It is a surface phenomenon. The adsorption process can occur at any interface such as liquid-liquid, gas-solid, gas-liquid, or liquid-solid, but liquid-solid interfaces of special interest from the water and wastewater treatment point of view. Basically, it is a surface phenomenon and adsorption takes place by physical forces but, sometimes, weak chemical bondings also participate in adsorption process (Faust and Aly 1983). A molecule (pollutant) adhered to the solid surface is called an adsorbate, and the solid surface as an adsorbent (Fig. 8.2).

The common adsorbents include activated carbon, molecular sieves, polymeric adsorbents, and some other low-cost materials. When adsorption is concerned, thermodynamic and kinetic aspects should be involved to know more details about its performance and mechanisms. Except for adsorption capacity, kinetic performance of a given adsorbent is also of great significance for the pilot application. From the kinetic analysis, the solute uptake rate, which determines the residence time required for completion of adsorption reaction. Further, the solid-liquid adsorption process is influenced by parameters such as pH, solubility of solute in the solvent, solution temperature and also the initial solute concentration. Furthermore, adsorption equilibrium is the set of conditions at which the number of molecules arriving on the surface of the adsorbent equals the number of molecules that are leaving. The relation between the amount of substance adsorbed by an adsorbent and the equilibrium concentration of the substance at constant temperature is called the adsorption isotherm (Theodore and Ricci 2010). In order to determine the adsorption isotherm several models have been suggested such as the Langmuir, Freundlich, Temkin, Elovich liquid film diffusion, intraparticle diffusion and Dubinin-Radushkevich isotherm models (Table 8.2). The applicability of the isotherm equation to the adsorption study done was compared by judging the correlation coefficients (R^2) (Tan et al. 2008).

8.3.1 Adsorption Kinetics

The study of adsorption kinetics is important because it provides valuable information and insights into the reaction pathways and the mechanism of the reactions (Table 8.3). An adsorption process is normally controlled by: (i) Transport of the solute from solution to the film surrounding the adsorbent, (ii) from the film to the

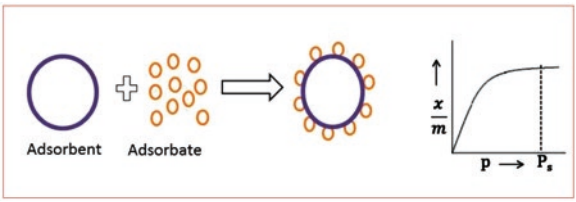

Fig. 8.2 Adsorption process

Table 8.2 Isotherm constant parameters and correlation coefficients calculated for various adsorption onto various adsorbent

Model type	Equation	Plot	Parameters
Langmuir	$\frac{1}{q_e} = \frac{1}{(K_a Q_m C_e)} + \frac{1}{Q_m}$	A plot C_e/q_e *Vs.* C_e exhibits straight line of slope $1/Q_m$ and an intercept of $1/(K_aQ_m)$	Q_m (mg g^{-1})
	$R_L = \frac{1}{1+K_l C_0}$	If R_L>1 unfavourable adsorption	K_a (L mg^{-1})
		R_L = 1 linear adsorption	R^2
		0<R_L<1 favourable adsorption and R_L=0 irreversible adsorption	
Freundlich	$\ln q_e = \ln K_F + (1/n) \ln C_e$	A plot ln (q_e) *Vs* ln (C_e) should be straight line	1/n
			K_F (L mg^{-1})
			R^2
Temkin	$q_e = B_1 \ln K_T + \ln C_e$	Values of B_1 and K_T were calculated from the plot of q_e *Vs.* ln (C_e).	B_1
			K_T (L mg^{-1})
		K_T is Temkin adsorption potential	R^2
		B_1 Temkin constant	
Dubinin and Radushkevich (D-R)	$\ln q_e = \ln Q_s - B\varepsilon^2$	The slope of the plot of ln (q_e) versus ε^2 and the intercept yields the adsorption capacity, Q_s (mg g^{-1}). ε is Polanyi potential (kJ mol^{-1})	Q_s (mg g^{-1})
			B
			ε (kJ mol^{-1})

adsorbent surface and (iii) from the surface to the internal sites followed by binding of analyte to the active sites. The slowest steps out of all the steps determine the overall rate of the adsorption process. There are different differential equations have been used for finding kinetic model in the batch system, these equations were solved by using integral method. If the kinetic model is correct, the appropriate plot of the concentration-time data should be linear (Do 1998). These include zero order, first order, second order, third order, pseudo first order, pseudo second order, parabolic diffusion and Elovich –Type.

Table 8.3 Kinetic parameters for the adsorption onto various adsorbent

Order of the reaction	Formula	Description
Zero order	Rate = $k[A]^0$	K is the rate constant of zero order adsorption (mg $L^{-1}min^{-1}$)
	Rate = k	
	$C_t = C_i - kt$	C_i and C_t are the liquid-phase concentrations of metal ions at initial and at time t, respectively (mg L^{-1})
First order	$\ln C = \ln C_i - K_1 t$	K_1 is the rate constant of first order adsorption (min^{-1})
Second order	$\frac{1}{C_t} = \frac{1}{C_i} + K_2 t$	K_2 is the rate constant of second order adsorption (L $mg^{-1}min^{-1}$)
Third order	$\frac{1}{C_t^2} = \frac{1}{C_i^2} + K_3 t$	K_3 is the rate constant of third order adsorption ($mg^2.L^{-2}$ min^{-1})
Pseudo first-order kinetic	$\log(q_e - q_t) = \log(q_e) - \frac{k_1}{2.303t}$	log ($q_e - q_t$) *Vs* t to give a linear relationship from which k_1 and q_e can be determined from the slope and intercept
Pseudo second order kinetic	$(t/qt) = \frac{1}{(k_2 q_e^2)} + \frac{t}{q_e}$	(t/q_t) *Vs* t to give a linear relationship from which k1 and q_e can be determined from the slope and intercept
Intraparticle diffusion	$q_t = K_{dif} t^{1/2} + C$	Values of K_{dif} and C were calculated from the slopes of q_t versus $t^{1/2}$
Elovich	$q_t = \frac{1}{\beta}\ln(\alpha\beta) + \frac{1}{\beta}\ln(t)$	Plot the values of q_t *Vs* ln (t) to give a linear relationship from which α and β can be determined from the slope and intercept, respectively
Describing the kinetics of heterogeneous	α and β are constants of Elovich –type equation.	q_t is concentration of adsorbate in solid phase at time (t).
Chemisorption	α represents the rate of chemisorption. β is related to the extent of surface coverage and the activation energy of chemisorption	

Table 8.4 Properties of nitrate and phosphate ions

Parameter	Nitrate	Phosphate
Molecular formula	NO_3^-	PO_4^{3-}
Charge	monovalent	Trivalent
Molar mass (g mol^{-1})	62.0049	94.97
Solubility in water (Na salts) (g L^{-1})	912.0 (25 °C)	88.0(25 °C)
Ionic radius (R_{ion}) ($\times 10^{-10}$ m)	3.0	–
Hydrated radius (R_{hyd}) ($\times 10^{-10}$ m)	5.1	3.39
Hydration free energy (ΔG_{hyd}) (kJ mol^{-1})	−305.85	–
Bulk diffusion coefficient, 25 °C (D_w) ($\times 10^{-9}$ m^2 s^{-1})	1.9	–

8.3.2 Batch and Column Experiments

The adsorption capability of adsorbent toward nitrate and phosphate anions can be investigated separately using aqueous solutions of KNO_3 and KH_2PO_4. Adsorption can performed batch-wise in Erlenmeyer flasks on a temperature regulated platform stirrer under the following parameters: temperature 25–55 °C, adsorbent dosage (g L^{-1}), pH 3–8, an initial concentration mg L^{-1} analyte ions. The pH of the solutions was adjusted by adding either 0.1 M HCl or 0.1 M NaOH. The adsorbent and anion suspensions were continuously agitated with a speed of optimized speed for particular time. In case, fixed-bed column studies will be performed using a laboratory scale glass column with an internal diameter of 1 cm and a length of 12 cm. A stainless sieve was attached at the bottom of column with a layer of glass wool. A known quantity of anion solution was fed in upwards through the column. The column was operated at three different flow rates ranging 0.5–1.5 mL min^{-1} for a solution concentration of 100 mg L^{-1}, a bed height of 12 cm, pH= 3–8, and 25 °C. Effluent samples were collected at the outlet of the column at regular time intervals and analyzed for anion concentration. The breakthrough curves were obtained by plotting the ratio (C/C_o) of anion concentration (C) at time (t) to initial concentration (C_0) versus time (t).

8.3.3 Physico-Chemical Properties of Nitrate and Phosphate

The adsorption mechanism of the nitrate and phosphate ions onto adsorbents is significantly dependent on the physico-chemical properties of N and P ions and their interaction with the adsorbent surface. Properties of nitrate and phosphate such as the solubility, ionic radius, hydration energy and bulk diffusion coefficient are crucial for the selective adsorption of these ions. These are compiled from different sources (Marcus 1997; Nightingale 1959; Richards et al. 2013; Custelcean and Moyer 2007; Kumar et al. 2014). Some of the important characteristics of inorganic anions are brief in Table 8.4.

The immobilization of anions onto the adsorbent also relies on the size of the adsorbent pores, which in some cases is similar or smaller than the ionic and/or hydrated dimensions of the anions. This hindrance results in selective anionic adsorption, and further results in the formation of inner-sphere, outer-sphere complexes and electrostatic or hydrogen bonding of the anion with the adsorbent surface. However, the differences in selective anionic adsorption cannot be adequately explained by the bare ionic radii, hydrated radii, stokes radii, diffusion coefficients or charge.

8.3.4 Nanoscience and Nanotechnology

Nanomaterials have a large surface area and high chemical reactivity compared to their corresponding bulk analogues and they can be fabricated in a variety of shapes and various lattice planes are present for reactions (Taniguchi et al. 1974). This is the most important and unique aspect about the nanomaterials for their end use in environmental remediation (Pradeep 2012). Also, nanomaterials are highly dispersible and can be anchored onto solid supports for desired applications and deployed in different environments (Ali 2012). These materials either transform contaminates to the harmless products chemically or adsorb/absorb onto the surfaces/cavities and hence removing/scavenging them (Bhattacharya et al. 2013; Pradeep 2009). The main aim in this review are to highlights recent advances in the development of novel nanoscale materials for removing nitrate and phosphate ions from water system. Figure 8.1 highlights four classes of nanoscale materials that are being evaluated as functional materials for water purification: (1) zerovalent metal-containing nanoparticles (ZVMNP), (2) nanoscale metal oxide materials (3) carbon based nanomaterials and (4) functionalized nanoscale materials. These have a broad range of physicochemical properties that make them particular attractive as separation and reactive media for water purification.

8.3.5 Nitrate and Phosphate Removal Using Nanoscale Zerovalent Materials

In comparison to larger sized ZVPs, nZVPs has a greater reactivity due to a greater surface area to volume ratio (Wang and Zhang 1997). Besides, nZVNP can be potentially used directly in the field for *insitu* treatment *via* injection at almost any location and depth in soil and groundwater systems (Chekli et al. 2016). Ideally, for this type of application, ZVNPs are expected to feature several key properties including: (i) high reactivity for the removal of targeted contaminants; (ii) high mobility in porous media; (iii) high reactive longevity after injection and (iv) low toxicity to the biota in the surrounding environment. These properties are the main tool when designing ZVNPs for water treatment (Yan

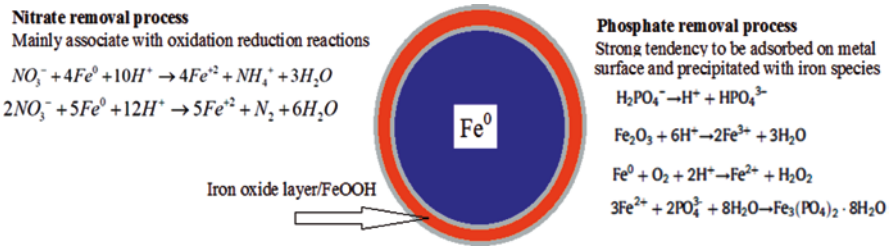

Fig. 8.3 Possible Mechanism of nitrate and phosphate removal using nZVI nanoprticles

et al. 2013). The most widely studied ZVNPs for environmental remediation is nanoscale zero-valent iron (nZVI). The synthesis of ZVI nanoparticles is relatively easy, involving the reduction of ferric ion by sodium borohydride (Wang and Zhang 1997). Typical groundwater contains many dissolved electron acceptors (nitrate or sulfate) that can react with nZVI surface and produce iron surface passivation (Fig. 8.3).

Moreover, nitrate removal is enhanced by lowering the pH by using either by adding acidic solutions or buffer system. However, addition of acidic solution like sulfuric acid (Huang et al. 1998), hydrochloric acid and acetic acid (Cheng et al. 1997) may be effective in lowering the pH but it also introduces species that has adverse impact on the quality of the drinking water. An alternative procedure to lower the pH is through the use of carbon dioxide bubbling (Ruangchainikom et al. 2006) since it can create an acidic environment by supplying the system with hydrogen ion (Hsu et al. 2004). Effect of both contaminant and solute concentrations on nZVI performance has been investigated in several studies (Table 8.5). On the other hand phosphate removal by NZVI and iron oxide nanoparticles is known to be a sorptive process, and the sorbed phosphate remains in the nanoparticles or sometimes get precipitated with iron species (Fig. 8.3).

Almeelbi and Bezbaruah 2012 have reported up to 100% removal of phosphate using nanoscale zero-valent iron (nZVI) particles and found nZVI particles to be more efficient than larger-sized particles (micro ZVI). Effectiveness of the NZVI in phosphate removal was found to 13.9 times higher than micro-ZVI (μZVI) particles with same nZVI and μZVI surface area concentrations used in batch reactors. A phosphate recovery better at higher pH and it decreased with lowering of the pH of the aqueous solution. The amount of nZVI in G-nZVI was an important factor in the removal of phosphorus by G-nZVI, and 20 % G-nZVI (20 % nZVI) would remove phosphorus most efficiently (Liu et al. 2014).

Further the specific reaction mechanism for the removal of phosphorus with nZVI or G-nZVI was mainly due to chemical reaction between nZVI and phosphorus. nZVI (Wen et al. 2014) was used to remove phosphate from aqueous solution, and the influence of pH, ionic strength and coexisting anions on phosphate removal. The results agree well with both Langmuir model and Freundlich model, and the calculated maximum adsorption capacity of phosphate was 245.65 mg/g. The removal of phosphate obviously decreased with an increasing pH due to the IEP of

Table 8.5 Performance of nZVNP for the removal of nitrate and phosphate pollutants

Adsorbent	Amount taken (mg/L)	pH and time (min)	Surface area (m^2/g)	Model and reaction rate	Adsorption capacity (mg/g)	Reference
nZVI	1–10	4	–	–	96–100 %	Almeelbi and Bezbaruah (2012)
		30			PO_4^{3-}	
G-nZVI	1–20	–	–	Freundlich	14.71	Liu et al. (2014)
		80			PO_4^{3-}	
nZVI	50–90	3–5	39.36	first order	63–98 %	Alessio (2015)
		60			NO_3^-	
nZVI	100	7	93.84	pseudo first-order kinetics	97 %	Hwang et al. (2011)
		90			NO_3^-	
nZVI	50	11	17.6	Langmuir-Hinshelwood	49.8	Kim et al. (2016)
		180		Pseudo first-order	NO_3^-	
nano-Fe/Cu	100	4	32.6	–	60 %	Hosseini et al. (2011)
		200			NO_3^-	
Cu–Pd/NZVI	30	7	–	first-order		Hamid et al. (2015)
		9 h				
nZVI	100	6–8	7.7	–	80–84 %	Hsu et al. (2011)
		5h			NO_3^-	
Nanoscopic Fe^0	50	3	39.36	first order kinetic	98 %	Biswas and Bose (2005)
		60			NO_3^-	
nZVI-graphite	100	6.7	6.18	–	80	Zang et al. (2006)
		30			NO_3^-	
nZVI – graphene	20	–	–	Freundlich	15.63	Peng et al. (2015)
		30			NO_3^-	
nZVI/Fe-Ag/EDTA	1000	4	48.13	–	340.15	Kunwar et al. (2012)
		240			NO_3^-	

nZVI. Alessio (2015) have reported an efficiency of nitrate removal up to 98 %, 87 % and 63 % were reached in 60 min during the treatment of solutions characterized by initial nitrate nitrogen concentrations of 50 mg/L, 70 mg/L and 95 mg/L, respectively and interaction was verified found to be a first order kinetic-type. nZVI prepared by chemical reduction without a stabilizing agent and possible mechanism between nitrate ion would be absorbed on the nZVI shell structure, and then the reduction reaction occurred on the shell structure by electron transfer from the core structure (Hwang et al. 2011). Moreover, the reduced ammonium ion would be isolated to the aqueous phase, and it was stripped to the gas phase under an alkaline condition. The nitrate reduction by nZVI is a heterogeneous catalytic reaction and it governs the pseudo-first-order and pseudo-second-order adsorption kinetic equations provided a good fit for the nitrate removal whereas the Langmuir-Hinshelwood kinetic equation provided a good fit for the ammonia generation (Kim et al. 2016).

nZVI particles supported on micro-scale exfoliated graphite were prepared by using KBH_4 as reducing agent in the H_2O/ethanol system (Zhang et al. 2006). The supported ZVI materials generally have higher activity and greater flexibility for nitrate removal to the extent of 80 % in the near neutral pH range.

Bimetallic of nano-Fe/Cu particles were synthesized and used in packed sand column experiments to reduce NO_3^--N through packed sand column (Hosseine et al. 2011). The rate of reduction by bimetallic particles is significantly faster than those observed for Fe^0 alone (Wang and Chen 1999). The mechanism responsible for this reactivity is related to catalytic hydrogenation and electrochemical effect (Tratnyek et al. 2003). In addition, a higher stability for the degradation and the prevention or the reduction of the formation and accumulation of toxic by products are the advantages of bimetallic nano particles. Nitrate removal using nZVI supported Cu−Pd bimetallic catalyst (Hamid et al. 2015) in a continuous reactor system. Advantages of their study was found to be higher removal efficiency, selectivity toward nontoxic products, relatively mild conditions, and easier operation compared to other physicochemical and biological technologies.

A small pilot scale study explored the capability of nitrate removal by nZVI particles in a re-circulated flow reactor of 4.3 L liquid volume (Hsu et al. 2011). Nitrate removal of 70 % was observed with the initial pH of 6.4 with the solution being pre-purged by N gas at a rate of 50 mL min^{-1}. The solution pH needs to be controlled within the neutral range to improve the nitrate removal by the nZVI process. In another report, nitrate-contaminated water passing through reactive porous media comprising of 125 cm^3 of sand containing 0.5, 1.0, or 1.5 g of steel wool and seeded with hydrogenotrophic denitrifying microorganism was sufficient to reduce nitrate concentrations from 40 mg/L as NO_3^--N to less than 2 mg/L as NO_3^--N with a retention time of 13 days (Biswas and Bose 2005). A mathematical model was developed to evaluate the performance of nZVI materials role in nitrate reduction, ammonium accumulation and hydrogen turnover (Peng et al. 2015).The simulation results further suggest a nZVI dosing strategy (3–6 mmol L^{-1} in temperature range of 30–40 °C, 6–10 mmol L^{-1} in temperature range of 15–30 °C and 10–14 mmol L^{-1} in temperature range of 5–15 °C) during groundwater remediation to make sure a low ammonium yield and a high nitrogen removal efficiency. EDTA/Fe-Ag nanohybrid material (Kunwar et al. 2012) used for nitrate removal and this interaction verify pseudo-first-order and pseudo-second-order adsorption kinetic equations. In addition, a Langmuir-Hinshelwood kinetic equation was able to successfully describe ammonia generation, apart from nZVI dose, the ionic strength, and effect of pH.

8.3.6 Nitrate and Phosphate Removal Using Nanoscale Metal Oxide Materials

Among the adsorbents used to improve water quality standards, hydrated metal oxides like Fe(III), Zr(IV), and Cu(II) have been more extensively explored for phosphate removal (Table 8.6) because they exhibit a strong ligand sorption (of HPO_4^{2-} and $H_2PO_4^-$) through the formation of inner sphere complexes and/or

Table 8.6 Performance of nano-scale metal oxide materials for the removal of nitrate and phosphate pollutants

Adsorbent	Amount taken (mg/L)	pH and time (min)	Surface area (m^2/g)	Model and reaction rate	Adsorption capacity (mg/g)	Reference
Bayoxide-E33	140	7.0 45	120–200	Langmuir model Intra-particle diffusion studies	38.8 PO_4^{3-}	Jacob et al. (2016)
Z-$La(OH)_3$	500	2.5–10.524 hr	55.69	Langmuir model pseudo-second-order reaction	71.94 PO_4^{3-}	Xie et al. (2014)
Fe–Mg–La	100	6.4 10 h	–	Langmuir model Intra-particle diffusion studies	48.3 PO_4^{3-}	Yu and Paul Chen (2015)
Fe–Al–Mn trimetal oxide	4.7–8.7	6.8 200 min	303	Freundlich model seudo-second-order	48.3 PO_4^{3-}	Lu et al. (2013)
Fe–Ti bimetal oxide	50	6.8 32 h	39.9	Langmuir model pseudo-second-order reaction	35.4 at pH 6.8. PO_4^{3-}	Lu et al. (2015)
n-HZO	10	6.8 6 h	2.34	Langmuir pseudo first- order	21.1 PO_4^{3-}	Chen et al. (2015)
n-$Mg(OH)_2$	10	6.0–12 80–100	–	Freundlich pseudo-first-order	45.6 PO_4^{3-}	Zhang et al. (2015)
Fe_3O_4/ZrO_2/chitosan	NO_3^-(100) PO_4^{3-} (50)	3 1440	212.9	Langmuir isotherm model	NO_3^- (89) PO_4^{3-}(26.5)	Jiang et al. (2013)
MgO- biochar	–	–	–	–	NO_3^- (94) PO_4^{3-} (835)	Zhang et al. (2012)
Fe–Zrbinary oxide	0–35	5.5 6 h	339	Langmuir model pseudo-second-order	PO_4^{3-} (33.4)	Ren et al. (2012)
CuO	200	5.5 180 min	200	Langmuir model Pseudo-second-order	PO_4^{3-} (23.9)	Mahdavi and Akhzari (2016)

through outer-sphere complexes (Chen et al. 2015). Batch, equilibrium, and column experiments were conducted by using Bayoxide E33 and its derivatives to determine various adsorption parameters (Jacob et al. 2016). Equilibrium data were fitted to different adsorption isotherms and the Langmuir isotherm provided the best fit. Based on the Langmuir model, it was found that E33/Ag II has a slightly higher maximum monolayer adsorption capacity (38.8 mgg^{-1}) when compared to unmodified E33 (37.7 mgg^{-1}). The uptake of phosphate by zeolite and lanthanum hydroxide (La-ZFA) was explained on the basis of the adsorption mechanism of the ligand exchange process (Xie et al. 2014). The sorbed phosphate could be recovered by hydrothermal treatment in 3 M NaOH at 250 °C, with a simultaneous regeneration of La-ZFA. The sorbent has a high phosphate removal capacity, with a sorption maximum of 71.94 mg/g, according to the Langmuir model. The removal of phosphate by La-ZFA performs well at a wide pH range, reaching > 95 % from pH 2.5 to pH 10.5 when initial P concentration < 100 mg/L. The sorbent Fe–Mg–La with Fe:Mg:La molar ratio of 2:1:1 ($Fe(NO_3)_39H_2O$, $MgSO_4H_2O$ and $La(NO_3)_36H_2O$) was prepared through co-precipitation approach for phosphate removal in contaminated water (Yang and Chen 2015). The hydroxyl groups play a key role in the phosphate removal by the sorbent and the presence of sulfate groups also play a certain role in the uptake. The spent sorbent can be successfully regenerated by 0.5 M NaOH solution. Yu and Chen 2015 have reported three different magnetic core–shell Fe_3O_4@LDHs composites, Fe_3O_4@Zn–Al–, Fe_3O_4@Mg–Al–, and Fe_3O_4@Ni–Al–LDH were prepared *via* co-precipitation method for phosphate adsorptive removal. The surface hydroxyl groups (M–OH) may well be exchanged by the adsorbed phosphate, forming outer-sphere surface complex (M–O–P). Therefore, the removal efficiency of phosphate was more than 80 % at pH 3–7. These magnetic core–shell Fe_3O_4@LDHs adsorbents may offer a simple single step adsorption treatment option to remove phosphate from water without the requirement of pre-/post-treatment for current industrial practice.

A nanostructured Fe–Al–Mn trimetal oxide synthesized by oxidation and co-precipitation method was reported (Lu et al. 2013). The phosphate removal gradually decreased with the increasing of pH (4–10.5). The phosphate adsorption on the adsorbent was fitted by Freundlich>Temkin>Langmuir at pH 6.8. The maximum adsorption capacity for Fe–Al–Mn trimetal oxide was about 48.3 mg/g at 25 °C. Spectroscopic analyses indicated that electrostatic attraction and replacement of surface hydroxyl groups (M\OH) by phosphate via the formation of inner-sphere complex were the main adsorption mechanism. The kinetics tests indicated that the phosphate sorption on Fe–Ti bimetal oxide at pH 6.8 obeyed the pseudo-second-order kinetics (Lu et al. 2015). The Langmuir sorption capacity for phosphate was 35.4 mg/g at pH 6.8. Spectroscopic analyses indicated that phosphate sorption on the Fe–Ti bimetal oxide occurred via replacement of surface hydroxyl groups (M-OH) by phosphate. The Fe–Ti bimetal oxide effectively regenerated by NaOH solutions. Nanosized hydrous zirconium oxide (HZO) supported by a macroporous anion exchanger D-201, exhibited highly preferable removal of phosphate from water even in the presence of other commonly occurring anions at greater levels (Chen et al. 2015). The exhausted HZO-201 can be in situ regenerated by

using a binary NaOH–NaCl solution for cyclic runs. A novel composite adsorbent (denoted as HMO-PN) by encapsulating active nano-$Mg(OH)_2$ onto macroporous polystyrene beads modified with fixed quaternary ammonium groups $[CH_2N^+(CH_2)_3Cl]$ (Zhang et al. 2015). The N^+-tailored groups can accelerate the diffusion of target phosphate through electrostatic attractions. Kinetic equilibrium of phosphate adsorption can be achieved within 100 min, and the calculated maximum adsorption capacity is 45.6 mg/g. Moreover, the exhausted HMO-PN can be readily regenerated using an alkaline brine solution. The Fe_3O_4/ZrO_2/chitosan composite used to adsorb both nitrate and phosphate (Jiang et al. 2013). Further, this was the first report of a modified chitosan with the ability to adsorb both of these two nutrient anions. The maximum adsorption amount of nitrate and phosphate is 89.3 mg/g and 26.5 mg P/g, respectively. The adsorption process fits well to the pseudo-first-order kinetic rate model, and the mechanism involves simultaneous adsorption and intra-particle diffusion.

Zhang et al. 2012 have developed porous MgO-biochar nanocomposites by crystallizing nano-MgO flakes in biochar matrix through slow pyrolysis of $MgCl_2$-pretreated biomass. This MgO-biochar nanocomposites exhibits an excellent adsorption ability to phosphates and nitrates in aqueous solutions. The Langmuir maximum capacity of phosphate on the MgO-biochar was around 835 mg/g, which is much higher than that of other adsorbents for the removal of phosphate from aqueous solutions. The Langmuir maximum nitrate capacity of MgO-biochar sample was around 94 mg/g. Performance of Fe–Zr binary oxide towards phopshate removal was established by Ren et al. 2012. The adsorption data fitted well to the Langmuir model with the maximum P adsorption capacity estimated of 24.9 mg P/g at pH 8.5 and 33.4 mg P/g at pH 5.5. The phosphate adsorption was pH dependent, decreasing with an increase in pH value. The presence of chloride, sulphate and carbonate doesn't interfere on phosphate removal. The phosphate uptake was mainly achieved through the replacement of surface hydroxyl groups by the phosphate species and formation of inner sphere surface complexes at the water/oxide interface. A nanoscale CuO material for the removal of phosphate by adsorption method (Mahdavi and Akhzari 2016). Equilibrium adsorption data for phosphate were in good agreement with Langmuir isotherms and pseudo-second-order equation indicating its chemisorption nature adsorption capacity was found to be 23.9 mg/g of CuO

8.3.7 Nitrate and Phosphate Removal Using Functionalized and Carbon Based Material

Carbon based materials like graphite, graphite oxide (GO), graphene, carbon nanotube (CNT), multiwall carbon nanotube (MWCNT), and functionalized carbon based materials have made potential applications in adsorption and catalysis. Only a few studies are reported for the removal of phosphate and nitrate ions from aqueous system (Table 8.7). The performance of carbon residue obtained as a by-product

Table 8.7 Performance of nano-scale carbon based materials for the removal of nitrate and phosphate pollutants

Adsorbent	Amount taken (mg/L)	pH and time (min)	Surface area (m^2/g)	Model and reaction rate	Adsorption capacity (mg/g)	Reference
Carbon residue	10	4 (NO_3^-) 6 (PO_4^{3-}) 5 hr	590	Langmuir model and pseudo-second-order	30.2 NO_3^- 11.2 PO_4^{3-}	Kilpimaa et al. (2015)
CNT	200	5.6 180 min	12.1	Freundlich Isotherms Pseudo-second-order kinetic	15.4 PO_4^{3-}	Mahdavi and Akhzari (2016)
GO/ZrO_2	20	6.0 48 h	160	Langmuir adsorption isotherms	16.45 PO_4^{3-}	Zong et al. (2013)
Graphene-FeOOH-Fe_2O_3	200	6 3 h	–	Freundlich model Second order equation	350 PO_4^{3-}	Diana et al. (2015)
Graphene	100	7	–	Langmuir Second order adsorption	89.37 PO_4^{3-}	Vasudevan and Lakshmi (2012)
MCM-48 silica	300	<8 NO_3^- 4–6 PO_4^{3-} 10	750	Freundlich model	NO_3^- (71 %) PO_4^{3-} (88 %)	Saad et al. (2007)
Zr(IV)-chitosan	NO_3^- (10) PO_4^{3-} (1000)	3–10 60	9.04	Langmuir and Freundlich	NO_3^-(128) PO_4^{3-} (149)	Sowmya and Meenakshi (2014)

from wood gasification process was employed as a precursor for preparing adsorbent by physical activation (Kilpimaa et al. 2015). The kinetics showed that the adsorption data followed pseudo-second-order kinetics and Langmuir model. This may be due to the homogeneous distribution of active sites on physically activated carbon residue and commercial activated carbon. Mahdavi and Akhzari (2016) have used CNT material for the removal of phosphate by adsorption method. Further, equilibrium adsorption data for phosphate were in good agreement with Freundlich sotherm and pseudo-second-order equation indicating its chemisorption nature adsorption capacity was found to be 15.4 mg/g of CNT. ZrO_2 functionalized graphite oxide by post-grafting method and employed it as a sorbent material for the removal of phosphate ions (Zong et al. 2013). Again, the adsorption capacity of phosphate ions on ZrO_2 functionalized graphite oxide was found to be highly dependent on the pH values and decreases on increasing the pH value from 2 to 12 and attained its maximum at a pH value of 2.03. This reduction in the adsorption capacity on increasing pH was explained on the basis of variation in the extent of various

types of interaction between phosphate ions and ZrO_2/graphene composite including electrostatic interaction, ion-exchange and acid base interaction. Phosphate removal based on graphene aerogel decorated with goethite (FeOOH) and magnetite (Fe_3O_4) nanoparticles (Diana et al. 2015). The aerogels showed a superior capacity to remove up to 350 mg g^{-1} at an initial phosphate concentration of 200 mg L^{-1} from aqueous system.

Graphene is an excellent phosphate adsorbent with an adsorption capacity of up to 89.37 mg/g at an initial phosphate concentration of 100 mg/L and temperature of 303 K (Vasudevan and Lakshmi 2012). The adsorption process follows second order kinetics, suggesting that the adsorption was a chemical controlling process. The adsorption of phosphate preferably fitting the Langmuir adsorption isotherm suggests monolayer coverage of adsorbed molecules. Effects of functional groups on the adsorption of $NO_3^-$and NO_2^- by carbon cloth (Afkhami et al. 2007). The carbon cloths were chemically etched in 4M H_2SO_4 solution after deionization cleaning procedure and used for the adsorption of NO_3^- and NO_2^- from water samples at nearly neutral (pH 7) solutions. Further, treatment of carbon cloth with acid produced positive sites on the carbon cloth, by protonation of surface –OH groups caused an increase in electrostatic adsorption of anions. The dramatic increase in the adsorption of anions by treatment of C-cloth with acid was attributed to the strong electrostatic interaction between the negative charge of anions and positive charge of the surface. The adsorption capacity of acid treated carbon cloth for $NO_3^-$and NO_2^- was 2.03 and 1.01 mmol/g, respectively. Powdered activated carbon (PAC) and carbon nanotubes (CNTs) were used for the removal of NO_3^- from aqueous solution (Namasivayam and Sangeetha 2005). The NO_3^- adsorption capacity of CNTs was found to be higher than PAC and decreased above pH 5. The equilibration time for maximum NO_3^- uptake was 60 min. Adsorption capacity of the PAC and CNTs was found to be 10 and 25 mmol NO_3^- per gram adsorbent, respectively.

The ordered mesoporous materials (OMM) with pore size between 2 and 50 nm were discovered in 1992 by researchers working for the Mobil Corporation. In 1998, researchers at the University of Califomia in Santa Barbara announced that they had produced silica with much larger 46–300 angstrom pores (Zhao et al. 1998) and latter the material was named Santa Barbara Amorphous type material (SBA-15). Surface modified mesoporous silica materials produced by surface functionalization *via* the tethering of organic functional groups are potential adsorbents used for removal of water pollutants. Saad et al. (2007) have reported 46 and 43 mgg^{-1} adsorption capacity when using ammonium functionalized MCM-48 for phosphate and nitrate ions removal, respectively. In another report (Saad et al. 2008), synthesized and protonated several amino-functionalized mesoporous silica materials and successfully applied them to remove nitrate from water. The aminated and protonated mesoporous silica showed high adsorption capacities of 0.6–2.4 mg g^{-1} for the unmodified mesoporous silica, despite the latter having a high surface area total pore volume. Phosphate was found to reduce nitrate adsorption, therefore, special types of functionalized mesoporous silicas (SBA-15) were produced where the nitrate adsorption was less affected by phosphate due to pore

size of adsorbent matching with nitrate ion. Unmodified cross-linked chitosan beads do not have the ability to remove nitrate and phosphate due to the absence of positive sites. Zr(IV) was loaded onto cross-linked chitosan beads to make the polymer selective towards the nitrate and phosphate anions (Sowmya and Meenakshi 2014). Zirconium based adsorbents have excellent anion adsorption capacities. Zr(IV) loaded sugar beet pulp was used for the removal of nitrate (Hassan et al. 2010), mesoporous ZrO_2 (Liu et al. 2008), amorphous zirconium hydroxide (Chitrakar et al. 2006) and Zr^{4+}introduced Mg-Al LDH (Chitrakar et al. 2007) were the various zirconium based materials reported for the removal of phosphate.

8.4 Conclusion

A critical evaluation of nanomaterials as adsorbents in this review article indicates that nanoparticles have been used for the removal of nitrate and phosphate species from water successfully. These nanocomposite materials are capable to remove pollutants even at low concentration, under varied conditions of pH and temperature. The dose required of nanoparticles is quite low, making their application economical. Moreover, it has been observed that the removal time is quite fast. These properties of nanoparticles made them ideal candidates for fast and inexpensive water treatment technology.

Acknowledgments Authors are thankful to the administration of VIT University, Vellore, India, for providing infrastructures to write this article and carry out other research.

References

Abou-Shady A, Peng C, Bi J et al (2012) Recovery of Pb (II) and removal of NO_3^- from aqueous solutions using integrated electrodialysis, electrolysis, and adsorption process. Desalination 286:304–315. doi:10.1016/j.desal.2011.11.041

Afkhami A, Madrakian T, Karimi Z (2007) The effect of acid treatment of carbon cloth on the adsorption of nitrite and nitrate ions. J Hazard Mater 144:427–431. doi:10.1016/j.jhazmat.2006.10.062

Alessio S (2015) Use of nanoscale zero-valent iron (NZVI) particles for chemical denitrification under different operating conditions. Metals (Basel) 5:1507–1519. doi:10.3390/met5031507

Ali I (2012) New generation adsorbents for water treatment. Chem Rev 112:5073–5091. doi:10.1021/cr300133d

Almeelbi T, Bezbaruah A (2012) Aqueous phosphate removal using nanoscale zero-valent iron. J Nanoparticle Res 14:1–14. doi:10.1007/s11051-012-0900-y

APHA (1985) Standard methods for examination of water and wastewater, 20th edn. American Public Health Association, Washington, DC

APHA (1998) Standard methods for examination of water and wastewater, 20th edn. American Public Health Association, Washington, DC

Bhattacharya S, Saha I, Mukhopadhyay A et al (2013) Role of nanotechnology in water treatment and purification: Potential applications and implications. Int J Chem Sci Technol 3:59–64

Biswas S, Bose P (2005) Zero-valent iron-assisted autotrophic denitrification. J Environ Eng 131:1212–1220

Chabani M, Amrane A, Bensmaili A (2006) Kinetic modelling of the adsorption of nitrates by ion exchange resin. Chem Eng J 125:111–117. doi:10.1016/j.cej.2006.08.014

Chekli L, Bayatsarmadi B, Sekine R et al (2016) Analytical characterisation of nanoscale zero-valent iron: a methodological review. Anal Chim Acta 903:13–35. doi:10.1016/j.aca.2015.10.040

Chen L, Zhao X, Pan B et al (2015) Preferable removal of phosphate from water using hydrous zirconium oxide-based nanocomposite of high stability. J Hazard Mater 284:35–42. doi:10.1016/j.jhazmat.2014.10.048

Cheng IF, Muftikian R, Fernando Q, Korte N (1997) Reduction of nitrate to ammonia by zero-valent iron. Chemosphere 35:2689–2695. doi:10.1016/S0045-6535(97)00275-0

Chitrakar R, Tezuka S, Sonoda A et al (2006) Selective adsorption of phosphate from seawater and wastewater by amorphous zirconium hydroxide. J Colloid Interf Sci 297:426–433. doi:10.1016/j.jcis.2005.11.011

Chitrakar R, Tezuka S, Sonoda A et al (2007) Synthesis and phosphate uptake behavior of Zr^{4+} incorporated MgAl-layered double hydroxides. J Colloid Interf Sci 313:53–63. doi:10.1016/j.jcis.2007.04.004

Custelcean R, Moyer B (2007) Anion separation with metal-organic frameworks. Eur J Inorg Chem 2007:1321–1340. doi:10.1002/ejic.200700018

Darbi A, Viraraghavan T, Butler R, Corkal D (2003) Pilot-scale evaluation of select nitrate removal technologies. J Environ Sci Health A Tox Hazard Subst Environ Eng 38:1703–1715. doi:10.1081/ESE-120022873

Diana NH, Shervin K, Luoshan W, Dusan L (2015) Engineered graphene–nanoparticle aerogel composites for efficient removal of phosphate from water. J Mater Chem A 3:6844–6852. doi:10.1039/c4ta06308b

Do DD (1998) Adsorption analysis: Equilibria and kinetics. Imperial College Press, London

Droste RL (1998) Endogenous decay and bioenergetics theory for aerobic wastewater treatment. Water Res 32:410–418. doi:10.1016/S0043-1354(97)00281-9

El Midaoui A, Elhannouni F, Menkouchi Sahli M et al (2001) Pollution of nitrate in Moroccan ground water: removal by electrodialysis. Desalination 136:325–332. doi:10.1016/S0011-9164(01)00195-3

El Midaoui A, Elhannouni F, Taky M et al (2002) Optimization of nitrate removal operation from ground water by electrodialysis. Sep Purif Technol 29:235–244. doi:10.1016/S1383-5866(02)00092-8

EPA (1990) Estimated national occurrence and exposure to nitrate/nitrite in public drinking water supplies. U.S. Environmental Protection Agency, Washington, DC, pp 2–32

EPA (2000) Wastewater technology fact sheet chemical precipitation. US Environmental Protection Agency, Washington, DC

Faust SD, Aly OM (1983) Chemistry of water treatment. Butterworth, Stoneham

Hamid S, Bae S, Lee W et al (2015) Catalytic nitrate removal in continuous bimetallic Cu – Pd/nanoscale zerovalent iron system. doi:10.1021/acs.iecr.5b01127

Hassan ML, Kassem NF, Abd El-Kader AH (2010) Novel Zr(IV)/sugar beet pulp composite for removal of sulfate and nitrate anions J. Appl Polym Sci 117(4):2205–2212. doi:10.1002/app.32063

Hayrynen K, Pongrácz E, Vaisanen V et al (2009) Concentration of ammonium and nitrate from mine water by reverse osmosis and nanofiltration. Desalination 240:280–289. doi:10.1016/j.desal.2008.02.027

Hell F, Lahnsteiner J, Frischherz H, Baumgartner G (1998) Experience with full-scale electrodialysis for nitrate and hardness removal. Desalination 117:173–180. doi:10.1016/S0011-9164(98)00088-5

Hosseini SM, Ataie-Ashtiani B, Kholghi M. (2011) Nitrate reduction by nano-Fe/Cu particles in packed column. Desalination 276:214–221. doi:10.1016/j.desal.2011.03.051

Hsu CY, Liao CH, Lu MC (2004) Treatment of aqueous nitrate by zero valent iron powder in the presence of CO_2 bubbling. Ground Water Monit Rem 24(4):82–87. doi:10.1111/j.1745-6592.2004.tb01305.x

Hsu J, Liao C, Wei Y (2011) Nitrate removal by synthetic nanoscale zero-valent iron in aqueous recirculated reactor. Sustain Environ Res 21:353–359

Huan Z (2006) Synthesis of nanoscale zero-valent iron supported on exfoliated graphite for removal of nitrate. Trans Nonferrous Metals Soc China 16:s345–s349

Huang CP, Wang HW, Chiu PC (1998) Nitrate reduction by metallic iron. Water Res 32:2257–2264. doi:10.1016/S0043-1354(97)00464-8

Hwang YH, Kim DG, Shin HS (2011) Mechanism study of nitrate reduction by nano zero valent iron. J Hazard Mater 185:1513–1521. doi:10.1016/j.jhazmat.2010.10.078

Jacob L, Han C, Li X, Dionysiou DD, Nadagouda MN (2016) Phosphate adsorption using modified iron oxidebased sorbents in lake water: kinetics, equilibrium, and column test. Chem Eng J 284:1386–1396. http://dx.doi.org/10.1016/j.cej.2015.08.114

Jenkins D, Ferguson J, Menar A (1971) Chemical processes for phosphate removal. Water Res 5:369–389

Jiang JQ, Graham NJD (1998) Pre-polymerised inorganic coagulants and phosphorus removal by coagulation – a review. Water SA 24:237–244

Jiang H, Chen P, Luo S et al (2013) Synthesis of novel nanocomposite Fe_3O_4/ZrO_2/chitosan and its application for removal of nitrate and phosphate. Appl Surf Sci 284:942–949. doi:10.1016/j.apsusc.2013.04.013

Kilpimaa S, Runtti H, Kangas T et al (2015) Physical activation of carbon residue from biomass gasification: novel sorbent for the removal of phosphates and nitrates from aqueous solution. J Ind Eng Chem 21:1354–1364. doi:10.1016/j.jiec.2014.06.006

Kim DG, Hwang YH, Shin HS, Ko SO (2016) Kinetics of nitrate adsorption and reduction by nano-scale zero valent iron (NZVI): Effect of ionic strength and initial pH. KSCE J Civ Eng 20(1):175–187. doi:10.1007/s12205-015-0464-3

Kraemer EO (1930) A Treatise on physical chemical chemistry. Taylor HS (ed) 2nd ed, vol II. D. Van Nostrand Co., Inc., New York

Kumar E, Bhatnagar A, Hogland W et al (2014) Interaction of anionic pollutants with Al-based adsorbents in aqueous media – a review. Chem Eng J 241:443–456. doi:10.1016/j.cej.2013.10.065

Kunwar PS, Arun KS, Shikha G (2012) Zero-valent bimetallic nanoparticles in aqueous medium. Environ Sci Pollut Res 19(9):3914–3924. doi:10.1007/s11356-012-1005-y

Lalley J, Han C, Li X et al (2016) Phosphate adsorption using modified iron oxide-based sorbents in lake water: kinetics, equilibrium, and column tests. Chem Eng J 284:1386–1396. doi:10.1016/j.cej.2015.08.114

Liu H, Sun X, Yin C, Hu C (2008) Removal of phosphate by mesoporous ZrO_2. J Hazard Mater 151:616–622. doi:10.1016/j.jhazmat.2007.06.033

Liu F, Yang J, Zuo J et al (2014) Graphene-supported nanoscale zero-valent iron: removal of phosphorus from aqueous solution and mechanistic study. J Environ Sci 26:1751–1762. doi:10.1016/j.jes.2014.06.016

Lu J, Liu H, Liu R et al (2013) Adsorptive removal of phosphate by a nanostructured Fe-Al-Mn trimetal oxide adsorbent. Powder Technol 233:146–154. doi:10.1016/j.powtec.2012.08.024

Lu J, Liu D, Hao J et al (2015) Phosphate removal from aqueous solutions by a nano-structured Fe–Ti bimetal oxide sorbent. Chem Eng Res Des 93:652–661. doi:10.1016/j.cherd.2014.05.001

Mahdavi S, Akhzari D (2016) The removal of phosphate from aqueous solutions using two nanostructures: copper oxide and carbon tubes. Clean Technol Environ Policy. doi:10.1007/s10098-015-1058-y

Marcus Y (1997) Ion properties. Dekker: New York: CRC Press

Namasivayam C, Sangeetha D (2005) Removal and recovery of nitrate from water by $ZnCl_2$ activated carbon from coconut coir pith, an agricultural solid waste. Indian J Chem Technol 12:513–521. doi:10.1016/j.chemosphere.2005.02.051

Nandita D, Ranjan S, Mundekkad D et al (2015) Nanotechnology in agro-food: from field to plate. Food Res Int 69:381–400. doi:10.1016/j.foodres.2015.01.005

Nightingale R (1959) Phenomenological theory of ion solvation. Effective radii of hydrated ions. J Phys Chem 63:1381–1387. doi:10.1021/j150579a011

Peng L, Liu Y, Gao SH et al (2015) Evaluation on the nanoscale zero valent iron based microbial denitrification for nitrate removal from groundwater. Sci Rep 5:12331. doi:10.1038/srep12331

Pfafflin JR, Ziegler EN (2006) Encyclopedia of environmental science and engineering, 5th edn, vol I and II. CRC Press, Boca Raton

Pradeep T (2009) Noble metal nanoparticles for water purification: a critical review. Thin Solid Films 517:6441–6478. doi:10.1016/j.tsf.2009.03.195

Pradeep T (2012) A text book of Nanosceince and Nanotechnology. Tata McGtaw Hill Edu Pvt. Lt, New Delhi

Rademacher JJ, Young TB, Kanarek MS (1992) Gastric cancer mortality and nitrate levels in Wisconsin drinking water. Arch Env Heal 47:292–294. doi:10.1080/00039896.1992.9938364

Razzaque MS (2011) Phosphate toxicity: new insights into an old problem. Clin Sci (Lond) 120(3):91–97. doi:10.1042/CS20100377

Ren Z, Shao L, Zhang G (2012) Adsorption of phosphate from aqueous solution using an iron–zirconium binary oxide sorbent. Water Air Soil Pollut 223:4221–4231. doi:10.1007/s11270-012-1186-5

Richards L, Vuachère M, Schafer AI (2010) Impact of pH on the removal of fluoride, nitrate and boron by nanofiltration/reverse osmosis. Desalination 261:331–337. doi:10.1016/j.desal.2010.06.025

Richards L, Richards BS, Corry B, Schafer AI (2013) Experimental energy barriers to anions transporting through nanofiltration membranes. Environ Sci Technol 47:1968–1976. doi:10.1021/es303925r

Ruangchainikom C, Liao CH, Anotai J, Lee MT (2006) Characteristics of nitrate reduction by zero-valent iron powder in the recirculated and CO_2 bubbled system. Water Res 40:195–204. doi:10.1016/j.watres.2005.09.047

Saad R, Belkacemi K, Hamoudi S (2007) Adsorption of phosphate and nitrate anions on ammonium-functionalized MCM-48: effects of experimental conditions. J Colloid Interf Sci 311:375–381. doi:10.1016/j.jcis.2007.03.025

Saad R, Hamoudi S, Belkacemi K (2008) Adsorption of phosphate and nitrate anions on ammonium-functionnalized mesoporous silicas. J Porous Mater 15:315–323. doi:10.1007/s10934-006-9095-x

Samatya S, Kabay N, Yüksel U et al (2006) Removal of nitrate from aqueous solution by nitrate selective ion exchange resins. React Funct Polym 66:1206–1214. doi:10.1016/j.reactfunctpolym.2006.03.009

Schlipkoter U, Flahault A (2010) Communicable diseases: achievements and challenges for public health. Public Health Rev 32:90–119

Schoeman JJ, Steyn A (2003) Nitrate removal with reverse osmosis in a rural area in South Africa. Desalination 155:15–26. doi:10.1016/S0011-9164(03)00235-2

Schumann U, Huntrieser H (2007) The global lightning-induced nitrogen oxides source. Atmos Chem Phys Discuss 7:2623–2818. doi:10.5194/acpd-7-2623-2007

Shivendu R, Dasgupta N, Chakraborty AR et al (2014) Nanoscience and nanotechnologies in food industries: opportunities and research trends. J Nanoparticle Res 16:2464. doi:10.1007/s11051-014-2464-5

Singh KP, Singh AK, Gupta S (2012) Optimization of nitrate reduction by EDTA catalyzed zero-valent bimetallic nanoparticles in aqueous medium. Environ Sci Pollut Res Int 19:3914–3924. doi:10.1007/s11356-012-1005-y

Sowmya A, Meenakshi S (2014) Zr(IV) loaded cross-linked chitosan beads with enhanced surface area for the removal of nitrate and phosphate. Int J Biol Macromol 69:336–343. doi:10.1016/j.ijbiomac.2014.05.043

Srinu NS, Setty YP (2011) Effect of carbon sources on biological denitrification of wastewater by immobilized *pseudomonas Stutzeri* bacteria in a fluidized bed bio reactor (FBBR). Int Proc Chem Biol Environ Eng 23:114–118

Tan IW, Ahmad L, Hameed BH (2008) Optimization of preparation conditions for activated carbons from coconut husk using response surface methodology. Chem Eng J 137:462–470. doi:10.1016/j.cej.2007.04.031

Taniguchi N, et al (1974) On the basic concept of nanotechnology. In: Proceedings of International Conference of Production Engineering Tokyo, Part II, Japan Society of Precision Engineering, pp 18–23

Theodore L, Ricci F (2010) Mass transfer operations for the practicing engineer. Wiley, New Jersey

Tratnyek PG, Scherer MM et al (2003) Permeable reactive barriers of iron and other zero-valent metals. In: Tarr MA (ed) Chemical degradation methods for wastes and pollutants: Environmental and Industrial Applications. Marcel Dekker, New York, pp. 371–421

Vasudevan S, Lakshmi J (2012) The adsorption of phosphate by graphene from aqueous solution. RSC Adv 2:5234. doi:10.1039/c2ra20270k

Wang CY, Chen ZY (1999) The preparation, surface modification, and characterization of metallic nanoparticles. Chin J Chem Phys 12:670–674

Wang CB, Zhang WX (1997) Synthesizing nanoscale iron particles for rapid and complete dechlorination of TCE and PCBs. Environ Sci Technol 31:2154–2156. doi:10.1021/es970039c

Wardlaw I (2012) Transport and transfer process in plants. Elsevier Science, Oxford

Wen Z, Zhang Y, Dai C (2014) Removal of phosphate from aqueous solution using nanoscale zerovalent iron (nZVI). Colloids Surf A Physicochem Eng Asp 457:433–440. doi:10.1016/j.colsurfa.2014.06.017

World Health Organization (1985) Health Hazards from nitrates in drinking water. World Health Organization, Copenhagen, pp. 73–94

World Health Organization (1997) Guidelines for drinking-water quality, Surveillance and control of community supplies, vol 3, 2nd edn. World Health Organization, Geneva

Xie B, Liu H (2009) Enhancement of biological nitrogen removal from wastewater by low-intensity ultrasound. Water Air Soil Pollut 211:157–163. doi:10.1007/s11270-009-0289-0

Xie J, Wang Z, Fang D et al (2014) Green synthesis of a novel hybrid sorbent of zeolite/lanthanum hydroxide and its application in the removal and recovery of phosphate from water. J Colloid Interface Sci 423:13–19. doi:10.1016/j.jcis.2014.02.020

Yan W L, Lien HL, et al (2013) Environ Sci Proc Imp 15:63–77

Yang Y, Chen JP (2015) Key factors for optimum performance in phosphate removal from contaminated water by a Fe-Mg-La Tri-Metal composite sorbent. J Colloid Interface Sci 445:303–311. doi:10.1016/j.jcis.2014.12.056

Yu Y, Paul Chen J (2015) Key factors for optimum performance in phosphate removal from contaminated water by a Fe–Mg–La tri-metal composite sorbent. J Colloid Interface Sci 445:303–311. doi:10.1016/j.jcis.2014.12.056

Zang H, Jin ZH, Han CH (2006) Synthesis of nanoscale zero-valent iron supported on exfoliated graphite for removal of nitrate. Trans Nonferrous Met SOC China 16:345–349

Zhang M, Gao B, Yao Y et al (2012) Synthesis of porous MgO-biochar nanocomposites for removal of phosphate and nitrate from aqueous solutions. Chem Eng J 210:26–32. doi:10.1016/j.cej.2012.08.052

Zhang Q, Zhang Z, Teng J, Huang H (2015) Highly efficient phosphate sequestration in aqueous solutions using nano-magnesium hydroxide modified polystyrene materials. Ind Eng Chem Res 2015(54):2940–2949. doi:10.1021/ie503943z

Zhao D, Huo Q, Feng J et al (1998) Nonionic triblock and star diblock copolymer and oligomeric sufactant syntheses of highly ordered, hydrothermally stable, mesoporous silica structures. J Am Chem Soc 120:6024–6036. doi:10.1021/ja974025i

Zong E, Wei D, Wan H et al (2013) Adsorptive removal of phosphate ions from aqueous solution using zirconia-functionalized graphite oxide. Chem Eng J 221:193–203. doi:10.1016/j.cej.2013.01.088